



HAL
open science

Simulation of Drawing of Small Stainless Steel Platinum Medical Tubes-Influence of the Tool Parameters on the Forming Limit

Camille Linardon, Jean-Sébastien Affagard, Grégory Chagnon, Denis Favier,
Benoit Gruez

► To cite this version:

Camille Linardon, Jean-Sébastien Affagard, Grégory Chagnon, Denis Favier, Benoit Gruez. Simulation of Drawing of Small Stainless Steel Platinum Medical Tubes-Influence of the Tool Parameters on the Forming Limit. THE 14TH INTERNATIONAL ESAFORM CONFERENCE ON MATERIAL FORMING: ESAFORM 2011, Apr 2011, Belfast, Ireland. 10.1063/1.3589553 . hal-01978919

HAL Id: hal-01978919

<https://hal.science/hal-01978919>

Submitted on 11 Jan 2019

HAL is a multi-disciplinary open access archive for the deposit and dissemination of scientific research documents, whether they are published or not. The documents may come from teaching and research institutions in France or abroad, or from public or private research centers.

L'archive ouverte pluridisciplinaire **HAL**, est destinée au dépôt et à la diffusion de documents scientifiques de niveau recherche, publiés ou non, émanant des établissements d'enseignement et de recherche français ou étrangers, des laboratoires publics ou privés.

Simulation of Drawing of Small Stainless Steel Platinum Medical Tubes - Influence of the Tool Parameters on the Forming Limit

Camille Linardon ^{a,b}, Jean-Sébastien Affagard ^{a,b}, Grégory Chagnon ^{b,*}
Denis Favier ^b, Benoit Gruez ^a

^a*Minitubes SA, 21 rue Vaujany, 38100 Grenoble, France*

^b*Laboratoire 3SR, UMR CNRS 5521, Université de Grenoble, BP 53, 38041 Grenoble Cedex 09, France*

**Corresponding author: gregory.chagnon@grenoble-inp.fr*

Abstract. Tube cold drawing processes are used to reduce tube diameters and thickness, while pulling them through a conical converging die with or without inner plug. An accurate modelling of the material deformation and friction behaviour is required in order to well describe these processes.

The study concerns a stainless steel platinum alloy. The material behaviour is characterised through tensile tests at strain rates as close as possible to the high strain rates reached during the drawing process. The results are fitted with an isotropic temperature-independent Johnson Cook constitutive equation. The modelling of floating plug drawing is performed on a ABAQUS/Explicit model. Friction coefficient is difficult to estimate with mechanical experimental tests, thus an inverse analysis is carried out to fit this parameter thanks to finite element simulation and experimental drawing tests. Drawing force measurements are recorded during the forming process. The Cockroft-Latham criterion is applied to understand the different process parameters influence on tube drawing and its accuracy for drawing process is evaluated.

Keywords: Tube drawing, Metal forming, Drawability, Johnson Cook, Cockroft & Latham.

PACS: 62.20.F

INTRODUCTION

Tube drawing is a forming process used to reduce tube section. The outer diameter reduction is controlled by a die while the inner diameter is controlled either by a mandrel or a floating plug depending on the tube dimensions as illustrated in figure 1. The interest of cold drawing compared to conventional hot drawing is its ability to obtain tubes with thin walls, good surface finish and enhanced mechanical properties. Dies are generally made of tungsten carbide for mandrel drawing and polycrystalline diamond (PCD) for floating plug drawing. In the industry, several drawing passes are always required to reach final tube dimensions. In order to reduce time consumption during processing it is important to know the maximum plastic deformation a tube can undergo. The modelling of tube drawing process was previously studied in [1]. The originality of this work is first the material of study, a steel platinum alloy, and its particular mechanical behaviour including strain rate dependency. Second it focuses on the floating plug drawing process and the concept of drawability limit is introduced. The tube drawability limit is linked to several parameters such as tube material, tools geometry, friction coefficient and strain rate. The drawability limit is reached when ductile fracture initiates in the tube and so relies on a failure criterion. Numerous theoretical failure criteria have been proposed to estimate the initiation of ductile fracture [2]. The aim of this study is to apply one of those criteria to estimate the drawability limits of tubes made of a stainless steel platinum alloy drawn on floating plug.

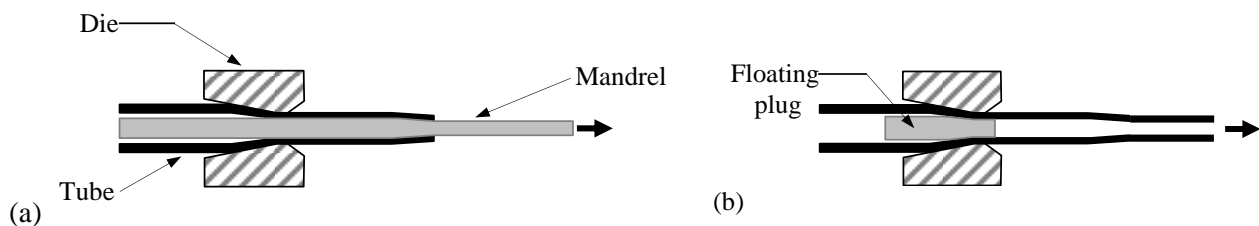


FIGURE 1. Drawing techniques: (a) mandrel drawing, (b) Floating plug drawing

MECHANICAL CHARACTERISATION

The tube drawing process is realised at various speeds depending on the passes. Thus the mechanical behaviour of the material must be known for different strain rates. In this way, tensile tests are performed on tubes.

Tube Tensile Tests

The tubes are 200mm long with an effective length of 100mm. Two mandrels are inserted at the edges of the tube in order to prevent deformation inhomogeneities. Industrial strain rates (up to 100s^{-1}) cannot be reached experimentally thus experimental tensile tests are performed at strain rates ranging from 0.005s^{-1} to 5s^{-1} . True stress versus true strain curves are plotted for each strain rate in figure 2. The curves highlight the strain rate dependency of stress and justify the use of a viscoplastic model.

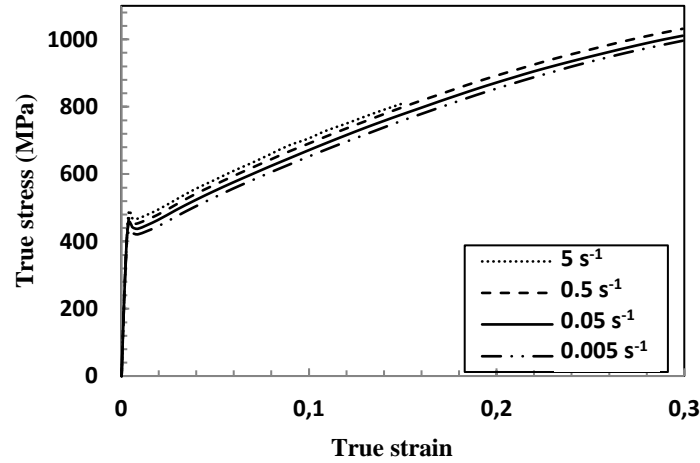


FIGURE 2. Stress-strain curves of tubes for different strain rates

Johnson Cook Plasticity Model

Most of the viscoplastic materials are greatly influenced by the temperature: a temperature increase is known to lower the admissible stresses. The Johnson Cook model [3] enables to model the strain rate dependence and the thermal softening:

$$\sigma_{eq} = (A + B\varepsilon_{eq}^n) \left(1 + C \ln \left(\frac{\dot{\varepsilon}_{eq}}{\varepsilon_{eq}^0} \right) \right) \left(1 - \left(\frac{T - T_0}{T_m - T_0} \right)^m \right) \quad (1)$$

where ε_{eq} is the equivalent plastic strain, $\dot{\varepsilon}_{eq}$ the equivalent plastic strain rate, T the current temperature, T_0 a reference temperature and T_m a reference melt temperature. A , B , C , n and m are material constants.

During the drawing process, it was observed [4] that temperature increase due to plastic deformation and friction would not exceed 100°C . According to Laheurte [5] and [4] thermal softening effects can be neglected and Johnson Cook model can be written as:

$$\sigma_{eq} = (A + B\varepsilon_{eq}^n) \left(1 + C \ln \left(\frac{\dot{\varepsilon}_{eq}}{\varepsilon_{eq}^0} \right) \right) \quad (2)$$

Determination of the Johnson Cook Material Parameters

The material Young's modulus is calculated from the elastic part of the stress-strain curves and set to 155 GPa. Poisson's ratio is supposed to be equal to 0.3. Due to the lack of information regarding the Poisson's ratio of the alloy, a sensitivity study about its influence on the simulation will be presented in a further part. The singularities observed at the beginning of the plastic zone on the stress-strain curve are identified as Lüders behaviour. Piobert [6] and Lüders [7] first reported the phenomenon of plastic strain localization observed in some alloys.

The material constant A represents the yield stress at temperatures below T_0 . The determination of the other parameters must be done considering that the Johnson Cook law cannot fit perfectly the experimental data. The errors between experimental data and Johnson Cook model must be minimised. In this study, the choice was made to minimise the errors for large deformations i.e. for strains larger than 0.2. The fitted parameters are detailed in Table 1. The fit of the model is presented in figures 3 and 4.

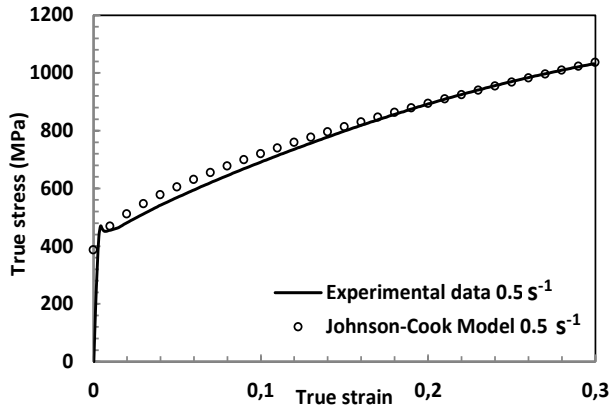


FIGURE 3. : Comparison of the stress calculated by Johnson Cook model and experimental values

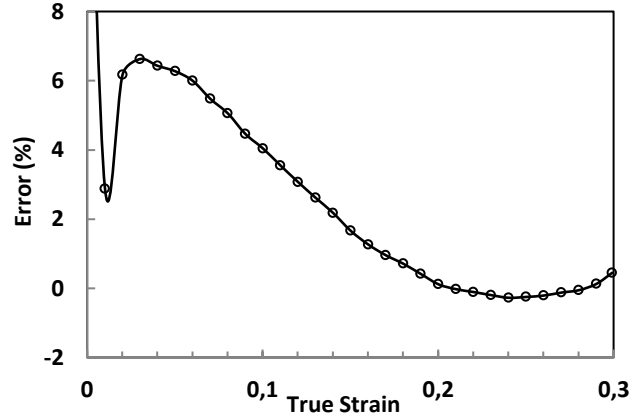


FIGURE 4. : Error between experimental data and Johnson Cook model

TABLE 1. Values of the Johnson Cook parameters for the stainless steel platinum alloy

A (MPa)	B (MPa)	C	n	$\dot{\epsilon}_{eq}^0$ (s^{-1})
376	1315	0.00597	0.608	0.005

MODELING OF DRAWING

The drawing process is studied through an ABAQUS Explicit model. The tube length is chosen long enough so that steady states conditions are reached. Die and floating plug are also modelled. The tube is considered to have a perfect coaxiality; thus the geometry of the model is simplified into an axisymmetric configuration as illustrated in figure 5. All the geometrical elements are meshed with four-noded linear elements with reduced integration. The stainless steel platinum alloy behaviour which is isotropic, viscoplastic, rate-dependent and temperature-independent is modelled by a Johnson Cook law. Die and floating plug materials are considered to be isotropic elastic, their Young's modulus are set to 950 MPa and 650 MPa respectively and the Poisson's ratio is equal to 0.2. All the thermal effects are neglected and the materials are modelled as temperature-independent. The model was validated thanks to surface temperature and drawing force measurements during experimental drawing tests.

The initial tube with dimensions of 1.80×2.07 mm is reduced to 1.39×1.60 mm. Simulations were done for several tools with different geometrical parameters which are presented in figure 6. Two different dies with semi-angle α and two different bearing lengths L were used. Concerning the floating plug, two semi-cone angles β with two different cone nose angles γ were used. All the parameters are listed in table 2, a total of 16 combinations of geometrical parameters were explored. The process is performed at ambient temperature at a drawing speed of 11.4 m/min.

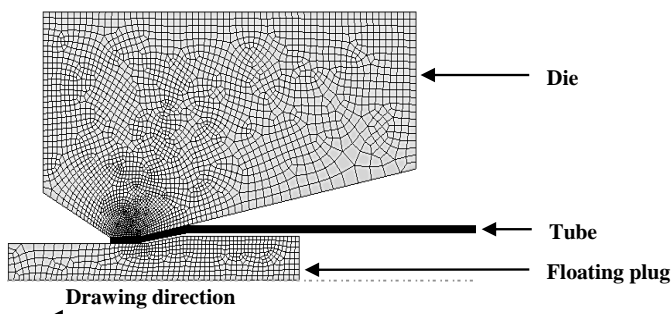


FIGURE 5. : Two-dimensional FE-model for tube drawing process

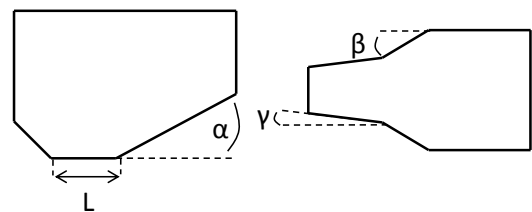


FIGURE 6. : Geometrical parameters of the die and the floating plug

TABLE 2. Values of the geometrical parameters of the tools

Die		Plug	
Semi cone angle	Bearing Length	Semi cone angle	Nose cone angle
α (°)	L (mm)	β (°)	γ (°)
12	0.16	10	0.17
19	0.56	17	1

SIMULATION ANALYSIS

Contact Modeling

Signorini [8] proposed a physical contact model for deformable bodies interacting with rigid static bodies. The contact is supposed to behave following a Coulomb friction law. Friction coefficient is dependent upon several parameters among which the most important are material roughness, interface temperature and lubricant. The influence of these parameters on friction behaviour is not easily identifiable and measurable. Thus friction coefficient values are determined by inverse analysis [1]. To carry out such an analysis a load cell is put at the die exit and drawing forces are recorded during drawing tests. Friction between tube/plug and tube/die are supposed to have the same characteristics.

A drawing force of 420 daN is experimentally measured during a drawing pass with a section reduction of 39%. A friction coefficient value is then chosen so that the simulated drawing force curve fits with the measured force. The value of 0,055 is allocated to the friction coefficient.

Parametric Study

Some of the material properties are determined with incertitude since only little information is available from literature and few experimental tests have been conducted on the alloy. Thus it is important to evaluate the model sensitivity towards those parameters to evaluate its accuracy.

Poisson's ratio is set to 0,3 according to values found in the literature. A variation of +/-16% around the mean value was investigated and reveals that the computed drawing force is not affected by such variations.

The variation of Young's modulus of +/-15% around the 155GPa value (determined through tensile tests) results in a variation of the stress distribution across tube wall and the average computed drawing force is unchanged.

TUBE DRAWABILITY

Cockroft-Latham Criterion Applied to Tube Drawing

The estimation of workability limits during tube drawing is of importance to understand the conditions leading to tube fracture during processing. Cockroft and Latham [9] established a criterion based on the observation that ductile fracture is more likely to occur in regions of largest tensile stress. The criterion is based on the calculation of a workability parameter $C_{process}$ defined as:

$$C_{process} = \int_0^{\varepsilon_f} \sigma_{max} d\varepsilon \quad (3)$$

where σ_{max} is the highest tensile principal stress, $d\varepsilon$ the equivalent plastic strain rate and ε_f the equivalent plastic fracture strain. When $C_{process}$ reaches a maximum value called C_{max} the material is likely to fracture. C_{max} is a material constant defined from the tensile stress-strain curve up to fracture (Fig. 7). The experimentally found C_{max} value for the stainless steel platinum alloy is 262 N.mm⁻².

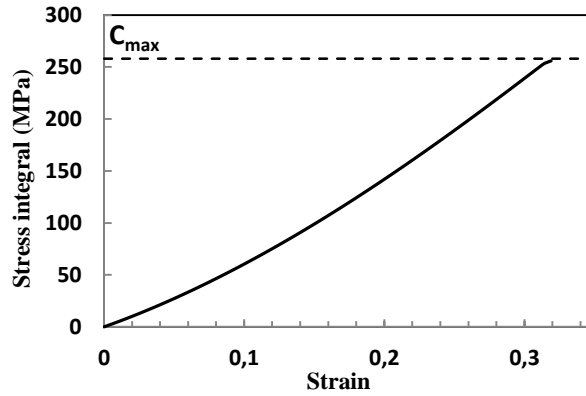


FIGURE 7. : Evaluation of $C_{process}$ during a tensile test and determination of C_{max}

Influence of the Die Geometry

Two geometrical parameters of the die are investigated: α and L . In a general way, $C_{process}$ values are higher for the nodes located on the outer surface. $C_{process}$ values are lower and more homogeneous for the nodes located on the inside of the tube (Fig. 8). The highest $C_{process}$ values on the external part of the tube are explained by greater material distortion and higher shear stress due to the die angle. Figure 8.a presents $C_{process}$ values computed for $\alpha=12^\circ$ and 19° respectively combined to $\beta=10^\circ$ and 17° . The other geometrical parameters are kept constant: $L=0.16$ mm and $\gamma=0.17^\circ$. A simultaneous increase of α and β leads to a more heterogeneous stress distribution through tube wall: inner stresses are lowered while outer stresses are increased. As a result, when increasing α and β the $C_{process}$ may exceed the C_{max} value and according to the Cockcroft-Latham criterion the drawability limit is reached. Fracture may initiate at the outer part of the tube and propagate inward. Figure 8.b presents $C_{process}$ values computed for $L=0.16$ mm and 0.56 mm, the other geometrical parameters are unchanged: $\alpha=12^\circ$, $\beta=10^\circ$ and $\gamma=0.17^\circ$. The die bearing length has little influence on the $C_{process}$. An increase of 350% of L (0.16mm to 0.56mm) results in a mean increase of 0.02% of the $C_{process}$ (Fig. 8.b).

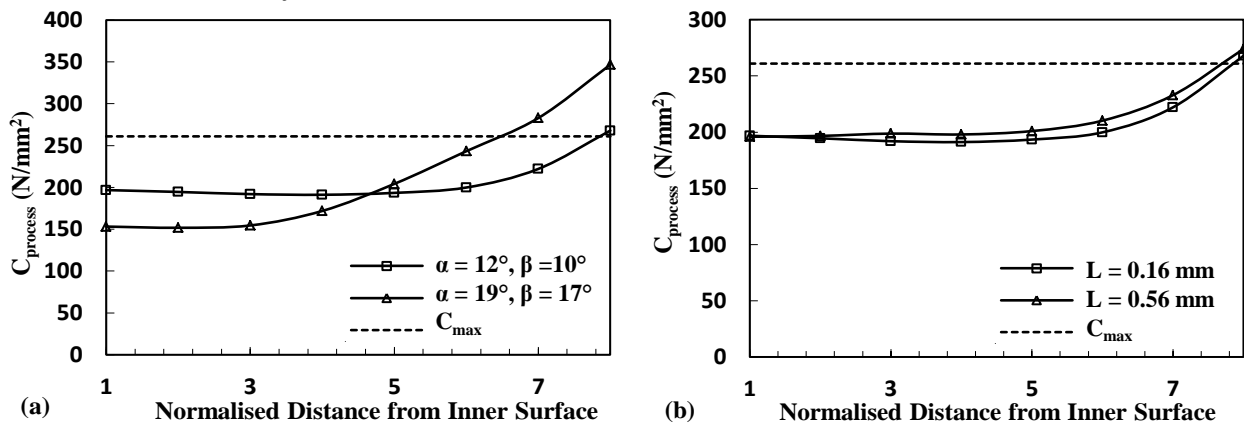


FIGURE 8. : Variation of Cockcroft-Latham ($C_{process}$) parameter along the tube thickness for (a) die semi-cone angle variation, (b) die bearing length variation

Influence of the Plug Geometry

The consequences of a plug nose cone angle variation depend on the die angle α (Fig.9). For $\alpha=12^\circ$ an increase of γ results in a translation of the plotted curves toward lower values of $C_{process}$ (Fig. 9.a). For $\alpha=19^\circ$ the consequences are slightly different: an increase in γ results in a decrease of the $C_{process}$ for the nodes located on the inside of the tube while the computed value for the external node is almost unchanged (Fig. 9.b). Thus the consequences of the variation of the plug nose cone angle are dependent on the die geometry and can hardly be predicted.

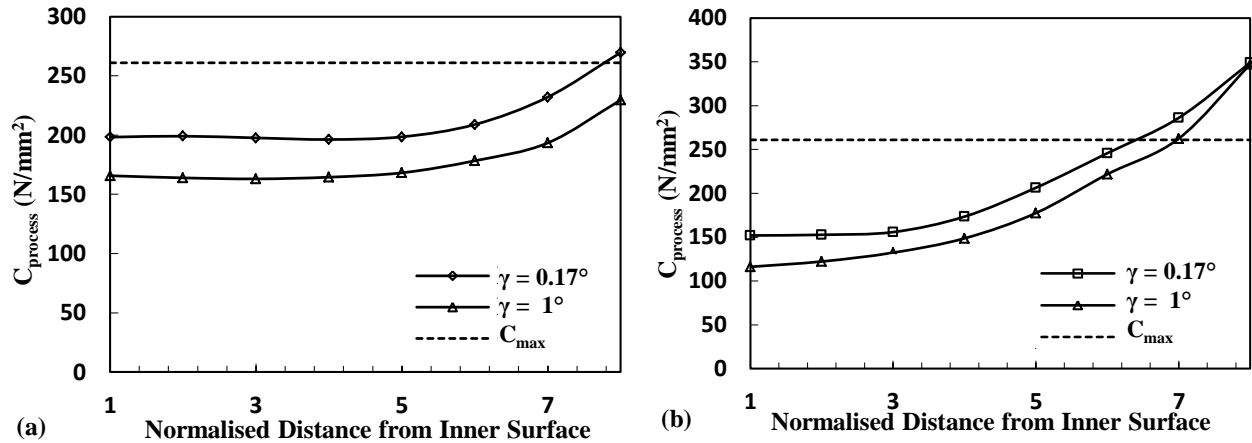


FIGURE 9. : Variation of Cockcroft-Latham ($C_{process}$) parameter along the tube thickness for a plug nose cone angle variation for a die with a semi-angle of (a) 12° and (b) 19°

CONCLUSION

Numerical methods such as FEM combined with failure criteria are expected to be a powerful tool to predict ductile fracture and formability limit for tube drawing. The Cockcroft-Latham criterion is not perfectly suited for tube drawing and other criteria should be explored for this special forming process. Nevertheless this parametric study permits to highlight the importance of small variation of the tools geometric parameters. To diminish the stress submitted to the tube it is important to use dies and plugs with small semi cone angles (12° and 10° respectively). A plug with higher nose cone angle e.g. 1° enables to lower the stresses in the tubes. Such a geometrical configuration permits to have a more homogeneous stress distribution across the tube wall and it lowers the risk of rupture.

REFERENCES

1. Palengat M., Chagnon G., Millet C., Favier D., Tube Brawing Process Modelling by a Finite Element Analysis, *NUMIFORM '07*.
2. Venugopal Rao A., Ramakrishnan N., Krishna kumar R., A comparative evaluation of the theoretical failure criteria for workability in cold forging, *Journal of Materials Processing Technology*, 142 (2003) 29–42.
3. Johnson, G.R., Cook, W.H., 1983. A constitutive model and data for metals subjected to large strains, high strain rates and high temperatures. *Proceedings of the Seventh International Symposium on Ballistic*, The Hague, The Netherlands, pp.541–547.
4. Palengat, M., “Modelisation des couplages multiphysiques materiaux-produits-procedes lors de l’etirage de tubes”, Ph.D Thesis, Grenoble Université, 2009
5. Laheurte, R., “Application de la théorie du second gradient a la coupe des matériaux”. Ph.D. Thesis, Université Bordeaux 1, 2004
6. Piobert, G., Morin, A.J., Didion, I., 1842. Commission des principes du tir. Memorial de l’artillerie. 5, 501–552.
7. Lüders, W., 1860. Über die äusserung der elasticität an stahlartigen eisenstaben und stahlstäben, und über eine beim biegen solcher stäbe beobachtete molecularbewegung. *Dingler’s Polytech. J.* 155, 18–22.
8. Signorini S., Sopra alcune questioni di elastostatica Atti della Societa Italiana per il Progresso delle Scienze, 1933.
9. Cockcroft M. G., Latham D. J., (1968), Ductility and the workability of metals. *Journal of the institute of metals* 96 pp, 33-39